AAS 26-602

APOLLO VS FNPEG ENTRY TERMINAL POINT GUIDANCE COMPARISONS FOR A MARS EDL MISSION

Lynn C. McGrew[*], Jeremy R. Rea[†], Breanna J. Johnson[‡‡]

The Apollo Entry Terminal Point Guidance algorithm has flown onboard Mars lander missions but requires significant parameter tuning. For future human to Mars missions, an operationally simpler yet robust guidance is desired, motivating evaluation of the Fully Numeric Predictor Corrector Entry Guidance (FNPEG) algorithm. For a representative Mars low L/D entry, descent and landing mission, Apollo and FNPEG were compared within an established 6 degree-of-freedom simulation. FNPEG improved terminal point precision, reducing downrange ellipse spread by about half, but also decreased terminal altitude by ~2 km, raising parachute deployment load concerns. A mid-point bank energy term may further refine FNPEG and recover altitude performance, similar to Apollo's bi-level reference trajectory approach.

INTRODUCTION

Entry Guidance was conceived and flown during the Apollo era, and the resulting Entry Terminal Point Controller algorithm coded into the onboard Guidance Navigation and Control (GNC) flight computer has provided the basis for other guidance schemes since. The final phase Apollo entry guidance was modified and successfully flown onboard the Mars Science Laboratory (Curiosity Rover) and Mars 2020 (Perseverance Rover) entry, descent and landing missions.[1,2] It was also augmented from a predictor-only to a predictor-corrector to fly onboard the Orion spacecraft as part of the Artemis I and II missions.[3]

While the Apollo Guidance Terminal Point Controller (TPC) algorithm heritage is robust, it is design-intensive and requires human-in-the-loop tuning of numerous parameters. Given a focus on human-to-Mars missions going forward, and interest in heavy and/or larger orbital assets in support of these missions and other scientific outer-planet endeavors, it is advantageous to simplify the guidance and control on the vehicle while maintaining robustness and improving performance. To meet this challenge, the Fully Numeric Predictor-Corrector Aerocapture Guidance (FNPAG) or Entry Guidance (FNPEG) algorithm is considered for its applicability across a wide range of vehicle ballistic coefficients and L/D, with little vehicle-dependent parameter tuning required.

Though many concept studies been performed using the FNPEG algorithm, it has yet to matured into a fully certified flight software product. To help advance the state of entry guidance technology, as well as operational robustness, a study was proposed during the early design phase

[*]Aerospace Engineer, Flight Mechanics & Trajectory Design Branch, NASA Johnson Space Center, Houston TX 77058.
[†]Guidance Technical Discipline Lead, Flight Mechanics & Trajectory Design Branch, NASA Johnson Space Center, Houston TX 77058.
[‡‡]Aerospace Engineer, Flight Mechanics & Trajectory Design Branch, NASA Johnson Space Center, Houston TX 77058.

of a representative Mars Sample Return mission to compare the performance of the Apollo and FNPEG algorithms. Given this mission's stringent landing dispersion performance requirements and the maturity of its 6 degree-of-freedom (6-DOF) simulation environment, this study also served to integrate FNPEG into the simulation model libraries and further its technology development potential into flight software applications

MARS ENTRY GUIDANCE

Design Considerations

Mission design must consider a variety of influencing factors, including entry flight-path angle and velocity, vehicle mass and aerodynamic characteristics (such as hypersonic ballistic coefficient and L/D), parachute deployment load constraints, the chute trigger type and altitude limitations, and key landing-site attributes such as latitude, season (Ls), and required uncertainty-ellipse size. Prior Mars lander missions provide extensive discussion of these design parameters.[4,5]

Navigation performance during entry is further constrained by reliance solely on IMU-derived accelerations, with no supplemental measurements of airspeed, altitude rate, or other aiding data to reduce state-estimation errors. As a result, both entry guidance and parachute deployment logic must operate within these limitations, and even ideal guidance cannot achieve a deploy-ellipse smaller than the navigation system's inherent position uncertainty.[6]

Altogether, the entry guidance system must be sufficiently robust to accommodate the significant uncertainties inherent in the Martian atmosphere. These uncertainties arise from both limited atmospheric observations and the highly variable, rapidly evolving nature of Mars' atmospheric dynamics, which makes accurate prediction challenging.[5]

Guidance Phases

A general overview of the Mars entry guidance phases is given in Figure 1. The operational concept begins with a Pre-Bank phase, which serves to command an attitude and bank command hold prior to the formal start of Entry Guidance itself. Range Control initiates the start of Entry Guidance where bank angle magnitude is used to minimize downrange error towards the target, as well as bank reversals used to manage crossrange error. Range Control then transitions to a Heading Alignment phase in order to use bank angle to mostly null out crossrange errors and maximize parachute deploy altitude. This prepares the vehicle for the final Straighten-Up-and-Fly-Right (SUFR) phase which levels and stabilizes the flight motion prior to parachute deploy. The parachute deploy point marks the terminal point target used for the entry guidance calculations.

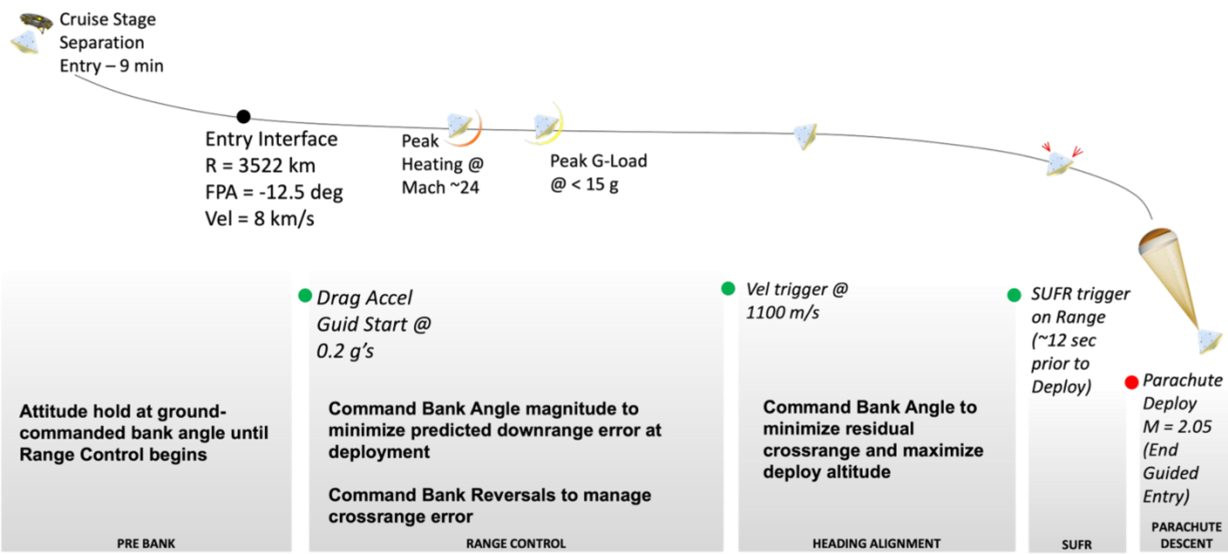

Figure 1. Mars Entry Guidance Phases

ALGORITHMS

Apollo

The Entry Terminal Point Controller (ETPC) used for the Mars missions represents the final phase of the Apollo Entry Guidance. The intricacies of its derivation and history are discussed in detail in papers by Graves (Reference 7) and Mosley (Reference 8), and its use on Mars missions.[9,10] Its purpose is to achieve safe deploy conditions while minimizing the total range error at the target. It does this by using bank angle to control downrange via range, altitude rate and drag acceleration from a stored reference trajectory. It does not try to follow this reference trajectory, rather just use the gains calculated from it to steer towards the target. For Apollo, this onboard reference trajectory takes the form of a look-up table as a function of velocity and is often represented as velocity vs bank angle or L/D to better understand the flown profile. Careful considerations must be made to shape these reference profiles.[1] Figure 2 illustrates the Apollo reference bank profile that was chosen for this representative mission and used for this analysis comparison.

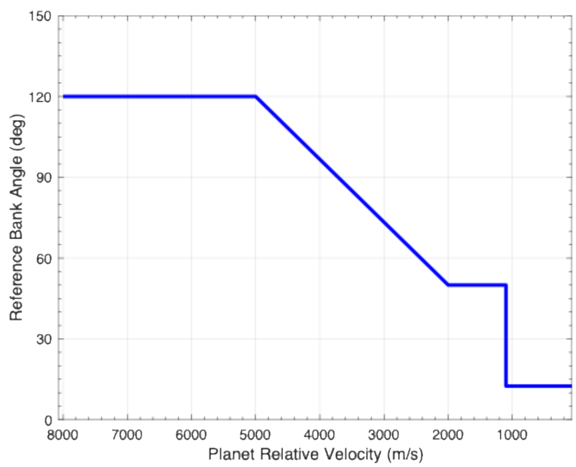

Figure 2. Example of the reference bank profile

Equation (1) represents the predicted range-to-go as a function of filtered drag and altitude rate errors with the corresponding partial derivative gains with respect to the nominal reference trajectory profile. The desired vertical component of the lift-to-drag ratio is a function of the difference between the actual and predicted range-to-go i.e. the downrange error in Equation (2). There is one minor modification in Eq. (2) compared to the original Apollo algorithm. The addition of chute deploy range bias constant R_{dep}, also called "Ranoff". This term represents an offset between the landing site and the chute deploy guidance terminal point target, as is used for ease of targeting operations. The difference is then converted to a change in commanded vertical L/D that is applied to the reference vertical L/D. An overcontrol gain term, K3, helps drive the necessary range error correction. The commanded bank angle is then calculated using the vertical L/D and the estimated L/D, along with a K2 term to denote the direction of the bank reversal, in Equation (3). Similarly, during the Heading Alignment phase, the commanded bank angle is proportional to the current azimuth error to the target, defined by the crossrange and downrange to the target, along with another overcontrol gain term K4, shown in Equation (4).

$$R_p = R_{ref} + \frac{\partial R}{\partial D}\left(D - D_{ref}\right) + \frac{\partial R}{\partial \dot{r}}\left(\dot{r} - \dot{r}_{ref}\right) \tag{1}$$

$$\left(\frac{L}{D}\right)_{V,C} = \left(\frac{L}{D}\right)_{V,ref} + \frac{K_3\left(R - R_p - R_{dep}\right)}{\partial R / \partial\left(L/D\right)} \tag{2}$$

$$\Phi_C = \cos^{-1}\left(\frac{L/D_{V,C}}{L/D}\right) * K_2 \tag{3}$$

$$\Phi_C = \tan^{-1}\left(\frac{R_c}{R}\right) K_4 \tag{4}$$

FNPEG

Where older guidance algorithms rely on pre-planned, set reference trajectories, the Fully Numeric Predictor-Corrector Entry Guidance (FNPEG) calculates the optimal path dynamically in real-time.

The algorithm was designed for flexibility, minimizing the number of tuning-parameter changes required across mission scenarios while providing a unified method applicable to vehicles spanning low to high L/D. It supports both skip and direct-entry trajectories without additional tuning, offers strong convergence through numerical root-finding methods such as Newton–Raphson, and is capable of enforcing complex aerodynamic-load and heating inequality constraints for Earth-entry applications.[11]

FNPEG continuously cycles through a two-stage numerical loop to drive targeting errors to zero. The independent energy variable the algorithm uses is expressed in Equation (5). Beginning with the predictor step the algorithm takes a current state vector (position, velocity, and altitude) and forward propagates them numerically using 3-degree-of-freedom (3-DOF) equations of motion to a user-defined final energy state, e_f, assuming a user-defined constant bank, σ_f, or linear bank profile, ($\sigma_f - \sigma_o$), with respect to energy, as depicted in Figure 3. Next, the corrector step compares this predicted downrange against the actual target constraints (such as a precise landing site). If that error is not converged, it then applies a root-finding technique to adjust the initial bank until the tolerance is achieved.

Once converged, the initial bank is output from the corrector as a bank command. Like Apollo, FNPEG uses magnitude of the bank angle to manage vertical lift, thus controlling the vehicle downrange. It also dictates the direction of the bank angle to manage crossrange via sign reversals; however, FNPEG has the capability to use numerically estimated crossrange to determine bank reversal timing. Additionally, FNPEG employs phugoid damping and g-load control, where small period oscillations and maximum peak g-loads can be constrained.[12]

$$e = \frac{1}{r} - \frac{v^2}{2} \tag{5}$$

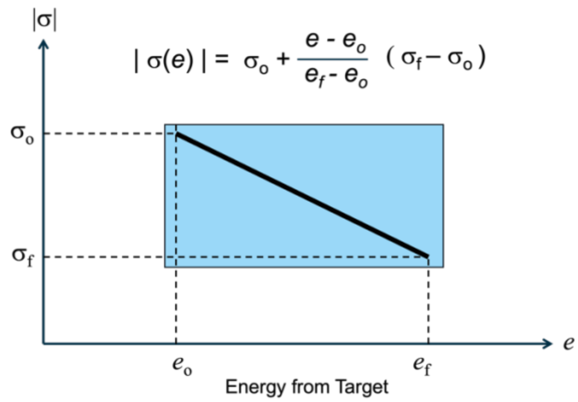

Figure 3. FNPEG Energy vs Bank Profile for Predictions

ANALYSIS APPROACH

Before undertaking the full 6-DOF analysis comparison, it was desired to prove the potential performance increase seen with a faster 3-DOF simulation comparison. This also helped identify where aspects of the two algorithms needed better functional alignment to enable fair performance comparisons. Since the Apollo guidance algorithm and functional control was the as-flown standard, several augmentations had to be made to the existing FNPEG analysis algorithm to better emulate those Apollo models.

The 3-DOF analysis was performed using the *Genesis* software simulation tool utilized at NASA Johnson Space Center[13] as this tool had already incorporated both the Apollo and FNPEG algorithms for previous studies of varying L/D and vehicle types, with the capability of handling nominal and dispersed Monte Carlo trajectories.

To simplify the analysis and remove additional sources of uncertainty in the comparison, navigation was assumed to be ideal (i.e. perfect navigation knowledge). For the initial 3-DOF analysis, MarsGRAM 2010 atmosphere and Mars Science Laboratory aerodynamics profiles were used for the density and speed of sound coefficient calculations.[14] The Apollo reference profile (as was shown in Figure 2) was pre-calculated and provided from an established entry trajectory. Both Apollo and FNPEG guidance control is initiated by a drag filter trigger set at 0.2g (Earth-g). The bank angle commands were passed to a proportional-derivative (PD) controller and effector emulator which modeled the rate and acceleration of the bank at 15 deg/s and 5 deg/s^2, respectively. Characteristics of the nominal profile trajectory are given in Table 1.

Table 1. Nominal Entry Trajectory Parameters

Trajectory Parameter	Value
Entry Flight Path Angle (inertial)	-12.5 deg
Entry Velocity	7.9 km/s
Range to Target	9.9 km
Target Altitude (detic)	9.4 km
Target Velocity (m/s)	525 m/s (SUFR) 463 m/s (Chute Deploy @ Mach 2.05)
Entry Mass, L/D	5400 kg, 0.29

Upon embarking on the 3-DOF analysis using *Genesis*, the following FNPEG algorithm augmentations were made to better match the Apollo models and improve performance outputs:

1. The lateral deadband model[15] used in the FNPEG predictor had to be updated to match the lateral deadband profile used in the Apollo-style guidance. The goal here was not to prove which crossrange control method was better for performance; rather to ensure that both algorithms were using the same model as to compare favorably. The Apollo-style uses a simple 2-step quadratic based upon velocity. When the lateral angle exceeds the deadband, a bank reversal is commanded.[8,9]
2. The predictor–corrector model incorporated the dynamics of bank reversals and the transition into the terminal (Heading Alignment) phase.
3. A time delta was added as a parameter input to freeze the active predictor-corrector guidance some number of seconds prior to the transition into the terminal phase (Heading Alignment). The predictor–corrector was observed to be struggling to converge just before the transition into the terminal phase.
4. The lateral angle definition in the terminal phase logic was used instead of delta azimuth as originally coded in FNPEG. This matches the Apollo-style guidance model.
5. Lift and drag acceleration factors were further refined by incorporating maximum-limit constraints and multiplicative bias terms—for example, informing the predictor that only 90% of the nominal lift is available—to preserve control authority later in the flight.
6. A parameter was added to specify a separate maximum bank angle for the predictor–corrector during the terminal phase. For instance, the predictor can assume full-lift-up throughout the Heading Alignment phase, thereby preserving maximum control authority during this phase.

Additional constraints levied on the dispersed performance of the Entry, Descent and Landing (EDL) have a profound impact on the design of entry guidance, namely the maximum g-load and parachute load limit requirements. For this mission, a peak g-load of 15g (Earth-g's) is a design requirement. The higher entry velocity also posed a challenge for this mission, requiring entry guidance to fly a lift-down early bank profile and perform its first bank reversal as an under reversal in order to avoid guidance saturation due to a greater sensitivity to altitude rate perturbations. The combination of g-load constraint, higher entry velocity, and higher ballistic coefficient also drove a shallower entry flight path angle than previous Mars landers recently. There is also a requirement on the landing ellipse uncertainty size which translates back to the errors in downrange and crossrange at the time of guidance termination. Although achieving those smaller ellipse sizes requires use of an alternative range-trigger[16], for the purpose of this study a velocity-trigger was employed at parachute deploy to better understand the effects of range error seen between the comparison of the algorithms.

The FNPEG augmentations were incorporated into the 3-DOF *Genesis* simulation were run for both closed-loop nominal and dispersed trajectories and compared to the both the original FNPEG and Apollo algorithms. For the 3-DOF FNPEG, a final bank angle $\sigma_f = 60^{O}$ was used but was not optimized for performance in this case. For the nominal trajectory in Figure 4, it can be seen that the augmented FNPEG displays a flight path that higher in its terminal altitude than the original algorithm and matches closer to the Apollo trajectory.

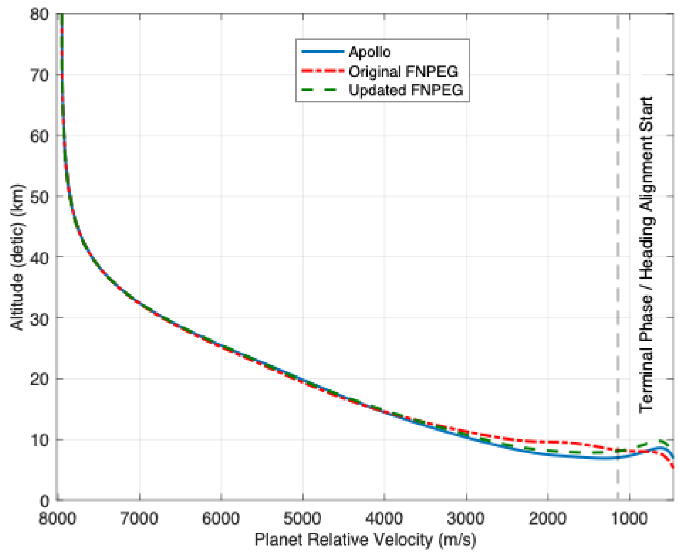

Figure 4. 3-DOF FNPEG algorithm improvement in nominal altitude

In Figure 5, the general behavior of the bank response seen in the augmented FNPEG is also more similar to the Apollo response than it is for the original FNPEG. The crossrange is generally improved, particularly near the start of the terminal (Heading Alignment) phase for FNPEG, seen in Figure 6. For the dispersed trajectories in Figure 7, there is a marked improvement in crossrange performance in the updated FNPEG over the original algorithm, as well as a distinct reduction in downrange spread in the FNPEG performance as compared with Apollo for the terminal ellipse. These observations confirmed that the FNPEG algorithm updates had validity in proceeding with 6-DOF simulation integration.

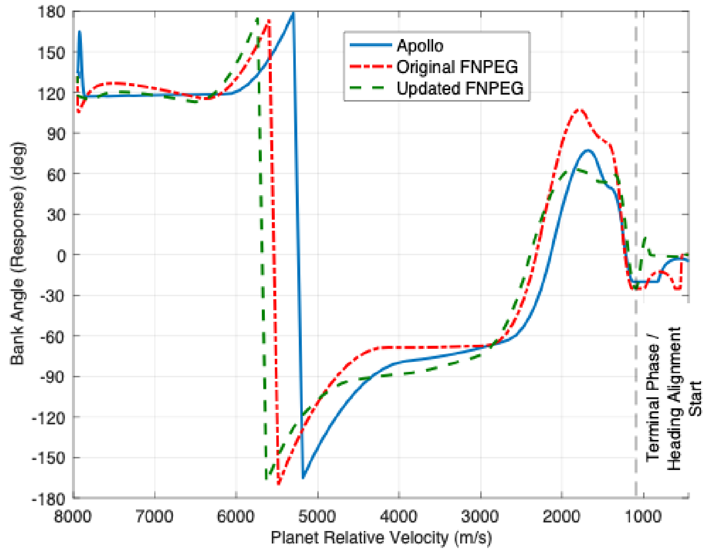

Figure 5. 3-DOF FNPEG algorithm comparison in nominal bank response

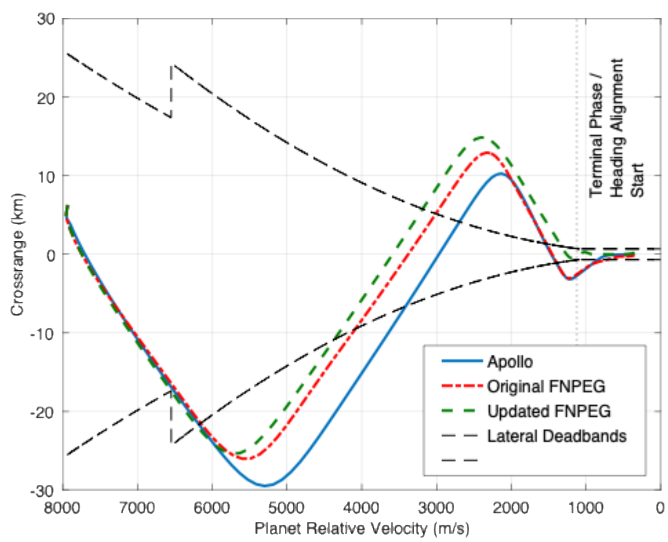

Figure 6. 3-DOF FNPEG algorithm comparison in nominal crossrange

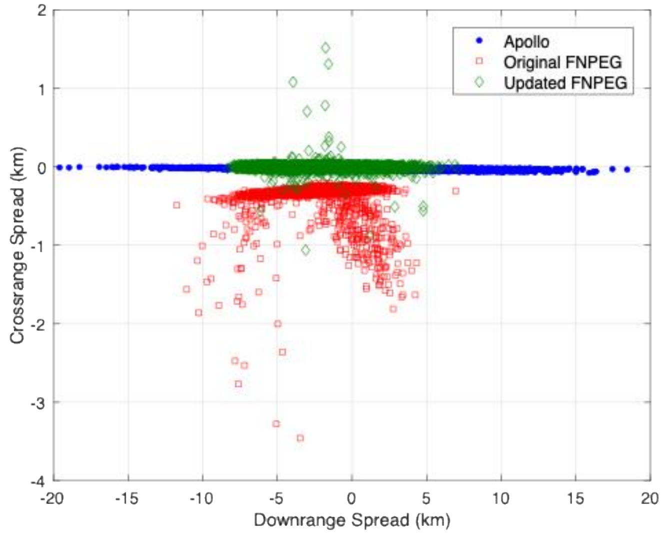

Figure 7. 3-DOF FNPEG algorithm comparison in terminal ellipse performance

RESULTS

For the 6-DOF algorithm comparison, the *Program to Optimize Spacecraft Trajectories II* (POST2) utilized at NASA Langley Research Center was used as the simulation environment, as it had the established multi-body vehicle, aerodynamic and mission-relevant mesoscale atmospheric models integrated for use.[17] For FNPEG, the density and speed of sound tabular data were curve-fit based upon a nominal of those aerodynamic and atmospheric models. As was done for the 3-DOF analysis, the navigation was assumed to be perfect, and the parachute deploy trigger was also based upon velocity.

While the FNPEG predictor-corrector utilized a fixed bank rate of 15 deg/s and bank acceleration of 5 deg/s^2 for its calculations, it should be noted that the vehicle control model itself uses a scheduled acceleration model based upon flight-regime phase to avoid reaction control system interactions. The vehicle model begins Range Control with a 2 deg/s^2 bank acceleration and increases to 3.5 deg/s^2 just prior to Heading Alignment; a bank rate of 20 deg/s is maintained throughout guided entry.

The updated FNPEG input parameters and values for this analysis are listed in Table 2. The lateral deadbands for the crossrange corridors remained unchanged from those for Apollo. The final bank was chosen such that it matched the late bank from the Apollo reference bank profile. The final altitude was chosen from the nominal Apollo closed-loop trajectory. The terminal phase, or Heading Alignment, was initiated by V_terminal at 1100 m/s, bounded by a maximum bank angle (sigma_max) of 25 deg, and with an overcontrol gain of 30 all identical to Apollo. Final velocity also proved to be a variable term depending on several factors but generally was adjusted until the resulting terminal Mach number was 2.05. The drag acceleration limit, Amax, is set at 15g to restrict the peak-g load during entry along with a controller gain term for enforcing this constraint, ka0. This controller gain had to be iterated upon until a desired drag acceleration and altitude performance was observed, similar to selecting a desired Apollo reference trajectory profile.

Table 2. Updated FNPEG Input Parameters

Trajectory Parameter	Value
Final Bank Angle	50 deg
Final Altitude	8500 m
Final Target Range	16378 m (SUFR to landing site target)
Final Velocity	525 m/s (SUFR) (Mach ~2.05 @ terminal point)
Amax	15 g
ka0	17
V_terminal	1100 m/s
sigma_max	25 deg
k_terminal	30
Time delta before terminal phase	5 sec
Lmax, Dmax factor	1.25, 1.25

The 6-DOF FNPEG trajectories in *POST2* confirm the behaviors observed in the 3-DOF trajectories from the *Genesis* simulation, yet exhibit notable differences compared to Apollo.

Figure 8 shows the nominal trajectory comparisons between the Apollo and FNPEG algorithms with respect to altitude as a function of velocity, both for the entirety of Entry and zoomed into the Heading Alignment phase. For FNPEG, trajectories both with and without the g-load constraint are compared. The Apollo trajectory exhibits a non-zero amount of lofting during the Heading Alignment phase, which appears to be advantageous for terminal point altitude in this case. Without the g-load constraint, there is lofting but the altitude falls more sharply to the terminal point, due to an increased flight path angle. When the g-load constraint is enforced in FNPEG, there is no lofting induced and the altitude is depressed by about 2 km as compared to the Apollo trajectory at the terminal point. Here, the g-load constraint appears to be restricting drag acceleration, thus suppressing the lift available for lofting (and therefore for increased altitude) to occur at the end of the terminal phase. While there is not an attitude requirement for this vehicle, an adequate amount of time is necessary to complete landing activities during the later powered descent phase post-parachute deploy, and that time combined with keeping parachute loads within specified parameters drives a need to maintain terminal altitude within a tight regime.

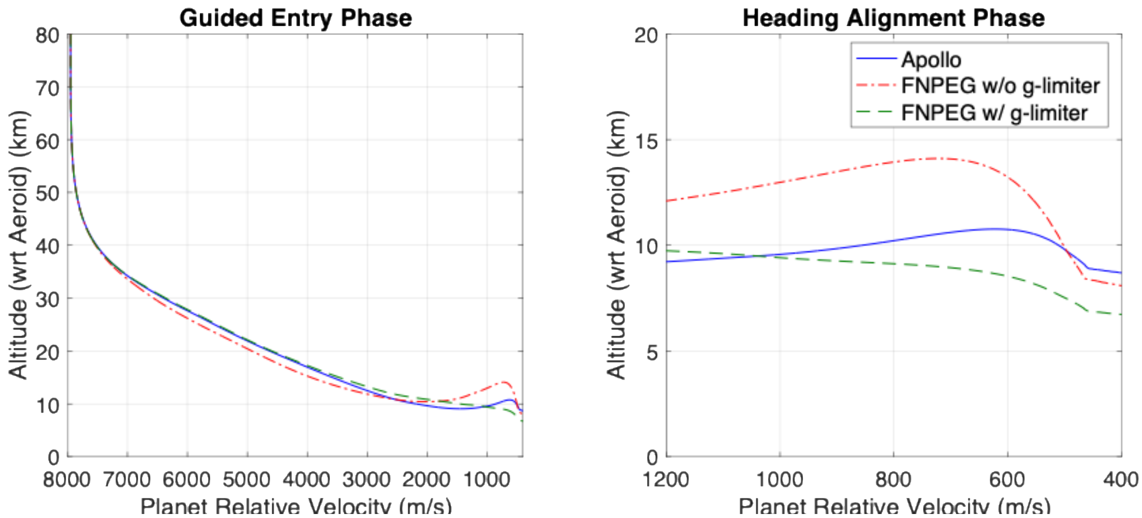

Figure 8. Nominal Trajectory Altitude Comparison between Apollo and FNPEG

Another algorithm trajectory comparison in nominal bank angle is observed in Figure 9. FNPEG sees a different bank command and response coming off the 1st reversal and into the 2nd reversal as compared to Apollo, due to the different peak-g and a g-load constraint imposed. Some of this bank response behavior can be attributed to the vehicle being at a different altitude, where variations in atmospheric density, speed of sound, and aerodynamic coefficients significantly influence performance predictions and feedback. Additionally, the Heading Alignment bank angle appears to drift away towards non-zero in the non-g-limiter FNPEG case, and saturates on the maximum bank allowed for much of the duration in the with g-limiter case, rather than settling around 0 deg as it does for Apollo. This remains an issue for future investigation to determine the cause of this behavior for FNPEG.

For the dispersed Monte Carlo trajectory algorithm comparison, Figure 10 charts the 99%-ile spread in downrange vs crossrange of the error ellipse at parachute deploy and normalized such that the ellipses are centered on the guidance terminal point. FNPEG improves landing precision with a downrange ellipse spread reduction of about 8 km or roughly half of the size of the ellipse, shrinking it from Apollo's 18 km to 10 km. The crossrange spread is fairly comparable between the two algorithms, which is expected given they are using identical lateral control schemes.

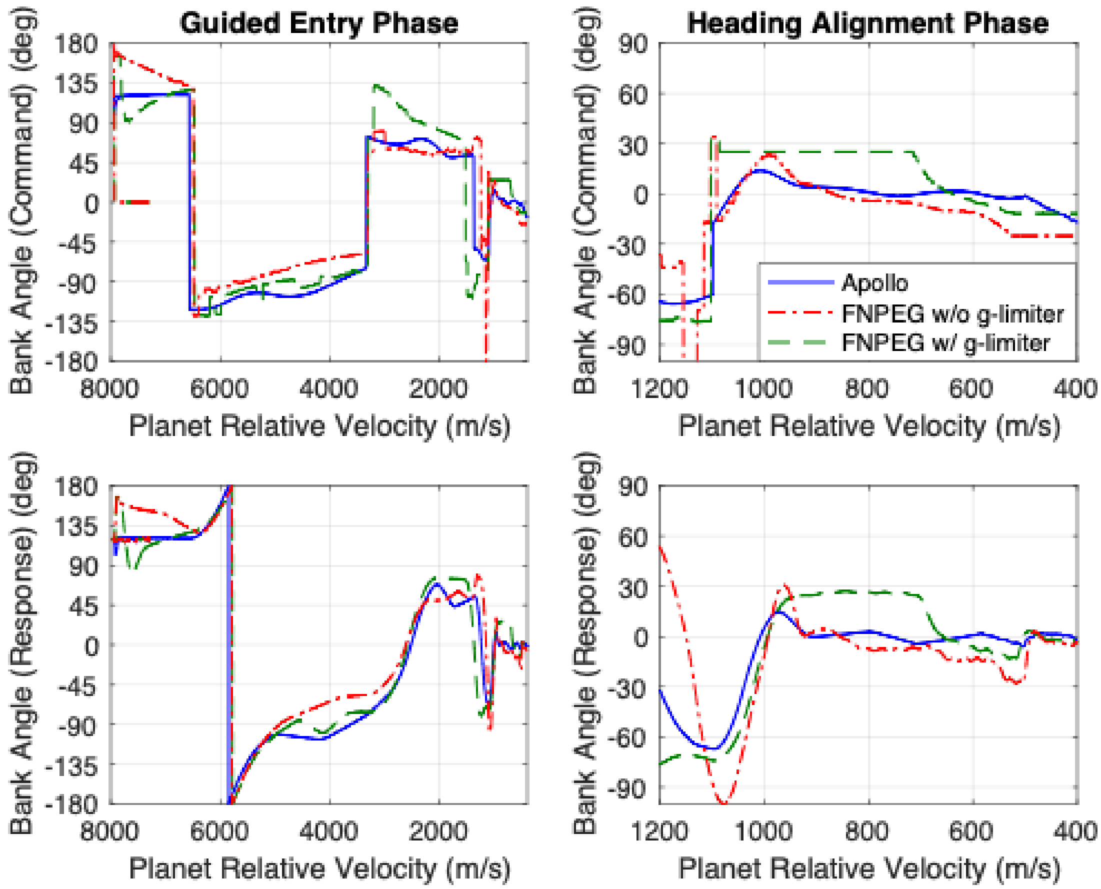

Figure 9. Nominal Trajectory Bank Angle Comparison between Apollo and FNPEG

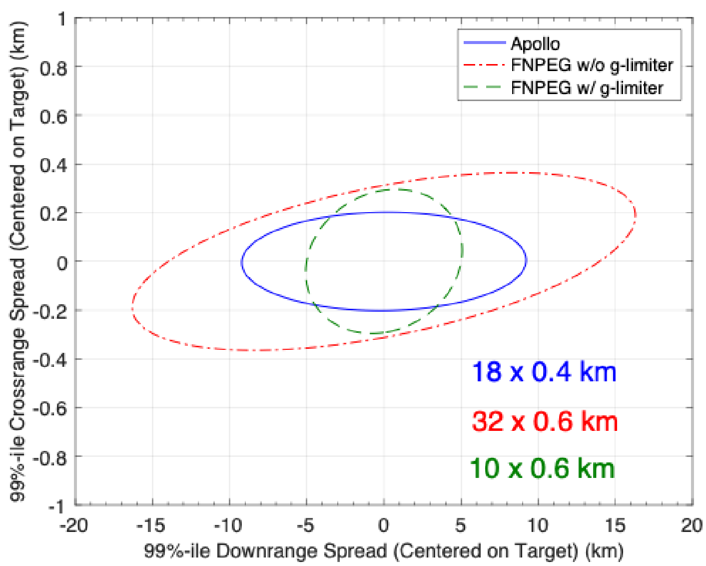

Figure 10. Dispersed Downrange vs Crossrange Error Ellipse (99%-ile) Comparison between Apollo and FNPEG

Attempts were made to adjust parameters such as final bank angle (σ_f), lift and drag factors and multipliers, and target altitude, but all had little to no effect on guidance trajectory performance in terms of its terminal altitude. It is surmised that this is due to the dominance of the g-load constraint, which limits drag acceleration and consequently reduces available lift for bank control, as the curves for g-load versus velocity illustrate in Figure 11. Additionally, adjusting the FNPEG guidance target uprange or downrange to affect the trajectory range-flown does not improve its terminal altitude performance and often worsens it, suggesting an analogous effect to g-load and lift limitations.

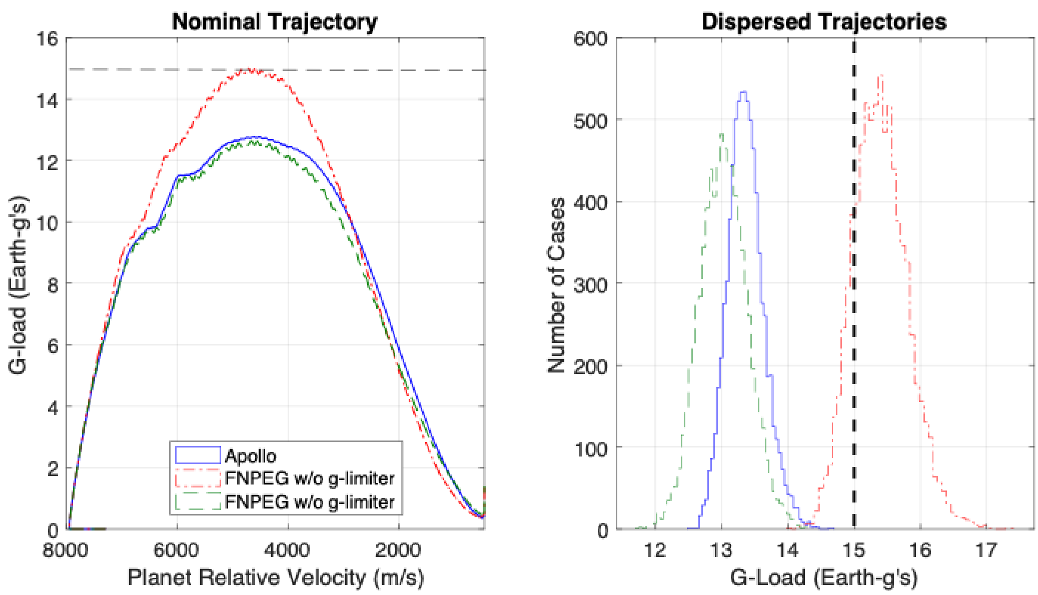

Figure 11. G-Load Comparison between Apollo and FNPEG (Nominal and Dispersed Trajectories)

CONCLUSION

The FNPEG algorithm was augmented to perform as much like the Apollo guidance algorithm as initially conceived for this representative Mars lander comparison study. While the FNPEG algorithm appears to perform as well or even better than Apollo in terms of downrange precision, there remains a question of whether its terminal altitude performance can be improved upon for this type of high entry velocity combined with highly constrained g-load type of Mars lander missions. It was found during the early design phases of Mars guided entry missions that a combination of higher ballistic coefficients and lower Martian atmospheric density warranted a bi-level approach to the bank profile shaping for the Apollo reference trajectory. When a heavier spacecraft design or thin Martian air degrades standard flight performance, switching to a variable bank profile recovers control. It lowers the vehicle's roll angle at slower speeds, keeping it flying longer in the dense lower atmosphere to maximize aerodynamic deceleration.

Therefore, it is the proposed subject of future work to introduce a possible mid-point energy and bank angle into the FNPEG predictor-corrector scheme to ascertain if this could improve terminal altitude performance without negatively impacting downrange precision, nor other desired performance metrics for these Mars entry and lander missions. Next steps also include accounting for navigation and controller interactions to better understand how 6-DOF effects impact the

FNPEG predictor-corrector terminal performance comparisons to those of Apollo for Mars entry, descent and lander missions.

ACKNOWLEDGEMENTS

This work is the result of ongoing efforts made by the development of the FNPEG algorithm by Dr. Ping Lu of San Diego State University. The task of getting the FNPEG code integrated into the 6-DOF Mars simulation and in working order was made possible by Pardha Sai Chadalavada of the Atmospheric Flight and Entry Systems Branch at the NASA Langley Research Center.

REFERENCES

[1]Mendeck, G.F., McGrew, L.C., "Post-Flight EDL Entry Guidance Performance of the 2011 Mars Science Laboratory Mission," AAS 13-419, AIAA Spaceflight Mechanics Conference, February 2013, Lihue, Kauai.

[2]McGrew, L.C., Killeen, B.J., "Entry Guidance Design and Post-Flight Performance of the Mars 2020 Mission," AAS 25-105, AIAA Spaceflight Mechanics Conference, January 2025, Lihue, Kauai.

[3]Putnam, Z.R., Neave, M.D., Barton, G.H., "PredGuid entry guidance for Orion return from low Earth orbit," IEEEAC 2010 1571, March 2010.

[4]Way, D.W., Powell, R.W., et. al., "Mars Science Laboratory: Entry, Descent, and Landing System Performance," IEEEAC 2007 1467, March 2007.

[5]Dutta, S., Karlgaard, C., Kass, D., Villar, G., and Mischna, M., "Post-flight Analysis of Atmospheric Properties from Mars 2020 Entry, Descent, and Landing," AIAA SciTech 2022, AIAA Atmospheric Flight Mechanics Conference, San Diego, CA, 2022.

[6]Serrichio, F., San Martin, A., Brugarolas, P., and Casoliva, J., "The Mars 2020 Perseverance Navigation Filter," AAS 21-539, AAS/AIAA Astrodynamics Specialist Conference, Big Sky, MT, 2021.

[7]Graves, C., Harpold, J., "Apollo Experience Report: Mission Planning for Apollo Reentry", MSC Internal Note No. 70-FM-155, October 5, 1970.

[8]Moseley, P.E., "The Apollo Entry Guidance: A Review of the Mathematical Development and its Operational Characteristics", TRW Note No. 69-FMT-791, December 1, 1969.

[9]Carman, G., Ives, D., Geller, D., "Apollo-Derived Mars Precision Lander Guidance", AIAA 98-4570, August 1998.

[10]Mendeck, G., Carman, G., "Guidance Design for Mars Smart Landers Using the Entry Terminal Point Controller," AIAA 2002-4502, AIAA Flight Mechanics Conference, August 2002, Monterey, CA.

[11]Lu, P.,"Entry Guidance: A Unified Method," Journal of Guidance, Control, and Dynamics, Vol. 37, No. 3, 2014, pp. 713–728.

[12]Lu, P., Brunner, C., Stachowiak, S., Mendeck, G., Tigges, M., and Cerimele, C.,"Verification of a Fully Numerical Entry Guidance Algorithm," Journal of Guidance, Control, and Dynamics, Vol. 40, No. 2, 2017, pp. 230–247.

[13]Murri, D. G., Matz, D. A., Hoffman, D. A., Berndt, J. S., Brown, S. C., and Prokop, L. E., "Improvements to the Flight Analysis and Simulation Tool (FAST) and Initial Development of the Genesis Flight Mechanics Simulation for Ascent, Aerocapture, Entry, Descent, and Landing (A2EDL) Trajectory Design," NASA/TM-20210014622, Apr 2021

[14]Schoenenberger, M., Dyakonov, A; et al, "Aerodynamic Challenges for the Mars Science Laboratory Entry Descent and Landing," AIAA 2009-3914. AIAA Thermodynamics Conference, San Antonio, TX June 23-25, 2009.

[15]Smith, K. M.,"Predictive Lateral Logic for Numerical Entry Guidance Algorithm," 26th AAS/AIAA Space Flight Mechanics Meeting, AAS Paper 2016-1182, 2016.

[16]Dutta, S, Way, D, "Comparison of the Effects of Velocity and Range Triggers on Trajectory Dispersions for the Mars 2020 Mission," AIAA SciTech Forum. Grapevine, Texas, Jan 2017.

[17]Way, D., Dutta, S; et al, "Assessment of the Mars 2020 Entry, Descent, and Landing Simulation," AIAA SciTech 2022, AIAA Atmospheric Flight Mechanics Conference, San Diego, CA, 2022.